International Journal of Engineering Research and Development
e- ISSN: 2278-067X, p-ISSN: 2278-800X, www.ijerd.com
Volume 22, Issue 8 (August 2026), PP 107-114

Polynomial Seventh-Order Two-Parameter Interpolation Kernel Optimization Using the Extended Slope Criterion

Zoran Milivojevic[1], Violeta Stojanovic[2], Dijana Kostic[2]
[1]*Department of Electrical and Computer Engineering, Engineering Academy of Serbia, Belgrade, Serbia,*
[2]*Department of Information-communication technology, Academy of Applied Technical and Preschool Studies, Niš, Serbia.*
Corresponding Author: Zoran Milivojevic

ABSTRACT
This paper presents the optimization of a polynomial seventh-order two-parameter (2P) interpolation kernel using the Extended slope criterion, obtained by extending the Slope criterion with an additional slope-equality condition. The Slope criterion requires the slope of the time-domain characteristic of the 2P kernel at the interpolation node $s = 1$ to be equal to the corresponding slope of the ideal $sinc$ kernel. Since this condition yields one equation with two unknown parameters, α and β, an infinite number of solutions is obtained. The criterion is therefore extended by imposing an additional condition requiring equality of the slopes at the interpolation node $s = 2$. The resulting system of two equations with two unknowns provides a unique pair of optimal parameters. In the spectral domain, the amplitude characteristic of the optimized 2P kernel, H, is compared with the ideal box-shaped characteristic, H_{sinc}, of the sinc kernel using similarity measures. The similarity measures include the total squared error, the slope in the transition band, and ripple characteristics represented by the peak-to-peak value, root-mean-square value, and ripple energy. The results demonstrate the spectral-domain performance of the optimized seventh-order 2P kernel and its similarity to the ideal sinc characteristic.
Keywords: *Convolution; interpolation; polynomial kernel; Amplitude characteristics; slope criterion.*

Date of Submission: 05-08-2026 Date of acceptance: 17-08-2026

I. INTRODUCTION

Interpolation is a fundamental operation in digital signal processing (DSP), enabling the estimation of signal values at positions between discrete samples [1], [2]. It is employed in a wide range of applications, including image, audio, and speech processing. In image processing, interpolation is required in spatial and geometric transformations, image rotation, and related operations [3], [4]. In speech processing, it is used in applications such as fundamental frequency estimation, speech synthesis, and the analysis of semantic and syntactic properties of speech [5]. The increasing use of interpolation in real-time DSP applications places simultaneous demands on interpolation accuracy and computational efficiency. Convolution-based interpolation provides an effective solution to these requirements by using an interpolation kernel, r, to determine the contribution of neighboring discrete samples to the interpolated value [6], [7]. Consequently, the properties of the interpolation kernel play a fundamental role in determining the accuracy and spectral characteristics of the resulting interpolation.

The ideal interpolation kernel is defined by the $sinc$ function, ($\mathrm{sinc}(x) = \sin(x)/x$), and is commonly referred to as the $sinc$ kernel. In the time domain, the $sinc$ kernel extends over an infinite interval $(-\infty, +\infty)$. Its amplitude characteristic corresponds to an ideal box-shaped frequency response, with a flat passband and stopband and an infinite slope at the transition. Since such an ideal interpolation kernel cannot be implemented directly in practical finite-length convolution-based systems, finite-length approximations of the $sinc$ kernel are required [8]. A straightforward approach is to truncate the $sinc$ kernel by applying a window function, w, thereby obtaining a finite-length windowed $sinc$ kernel suitable for practical interpolation. However, windowing modifies the ideal spectral characteristic and introduces ripple in the passband and stopband, while the transition between the passband and stopband becomes gradual, with a finite slope. These deviations from the ideal $sinc$ characteristic motivate the development of finite-support interpolation kernels with improved time- and frequency-domain properties. In particular, the design of a finite-length kernel of length L and appropriate shape that provides a close approximation to the ideal $sinc$ kernel remains an important problem in convolution-based interpolation.

Polynomial interpolation kernels of relatively low order, $n \leq 7$, have been developed as finite-length approximations of the $sinc$ kernel. The zeroth-order kernel represents the simplest case, in which the interpolated value is determined from the nearest-neighbor sample. Although this approach provides very high computational efficiency, its interpolation error is relatively large. Higher-order polynomial kernels, including linear ($n = 1$), cubic ($n = 3$), quintic ($n = 5$), and seventh-order ($n = 7$) kernels, provide progressively improved interpolation accuracy [2], [9]. In particular, one-parameter (1P, α) polynomial kernels allow their time- and spectral-domain characteristics to be adjusted through the parameter α, providing the possibility of optimizing the kernel according to a selected criterion. The seventh-order 1P kernel represents a high-order polynomial formulation within this class and provides a basis for further extension through the introduction of an additional independent parameter.

To achieve greater flexibility in adapting the interpolation kernel to the characteristics of a specific signal, two-parameter (2P, α, β) interpolation kernels have subsequently been developed. The third-order 2P kernel was first proposed in [10], followed by the development of a fifth-order 2P kernel in [11]. In [12], a polynomial seventh-order two-parameter (2P, α, β) interpolation kernel was constructed in accordance with the requirements that an interpolation kernel must satisfy, primarily concerning the similarity between the time-domain characteristics of the 2P kernel and the $sinc$ kernel at all interpolation nodes [13]. To satisfy these requirements, a system of 38 equations with 40 unknowns was first formulated. Two coefficients were then defined as the kernel parameters α and β, thereby parameterizing the kernel and providing an unambiguous solution to the system of equations.

In this paper, the seventh-order polynomial 2P interpolation kernel is optimized according to the Slope criterion [8]. The Slope criterion requires the slope of the time-domain characteristic of the 2P kernel at the interpolation node $s = 1$ to be equal to the corresponding slope of the ideal $sinc$ kernel. The optimization procedure leads to a single equation with two unknown parameters, α and β. Consequently, an infinite number of parameter pairs (α, β) satisfy this equation, which in the (α, β) plane forms a straight line. To obtain a unique solution, the Slope criterion is extended by introducing an additional condition, requiring equality of the slopes at the interpolation node $s = 2$. This Extended slope criterion results in a system of two equations with two unknowns, whose solution determines the optimal kernel parameters, α_{opt} and β_{opt}. Following the notation used for the optimal parameter of the 1P kernel [8], the optimal parameters of the 2P kernel are denoted in this paper as $\alpha_\zeta = \alpha_{opt}$ and $\beta_\zeta = \beta_{opt}$. In the second part of the paper, a comparative analysis of the optimized seventh-order 2P kernel is performed against the optimized seventh-order 1P kernel, whose optimal parameter was determined according to the Slope criterion, and the non-parametric $sinc$ and windowed $sinc$ kernels, $sincw$. The $sincw$ kernel is obtained by windowing the $sinc$ kernel with a rectangular (box) window of length $L_w = 10$. The comparison is performed in the spectral domain by analyzing the amplitude characteristics using the following similarity measures: the total squared error E_T, the slope of the spectral characteristic k_H in the transition band, and the ripple characteristics, including the peak-to-peak value $H_{r,pp}$, the root-mean-square value $H_{r,rms}$, and the ripple energy E_r. The results of the comparative analysis are presented graphically and in tabular form.

The remainder of this paper is organized as follows. Section II presents the definition of the seventh-order polynomial 2P interpolation kernel. Section III describes the optimization of the 2P kernel using the Extended slope criterion. Section IV presents a comparative analysis of the optimized 2P kernel in the spectral domain. Section V concludes the paper.

II. POLYNOMIAL SEVENTH-ORDER 2P INTERPOLATION KERNEL

In [13], the construction of a polynomial seventh-order one-parameter (1P) convolutional interpolation kernel was presented. The seventh-order two-parameter (2P) interpolation kernel was developed based on the seventh-order polynomial one-parameter (1P) kernel described in [12]. The main objective of the proposed 2P kernel is to provide a more accurate approximation of the ideal $sinc$ interpolation kernel over the interval $(-5, 5)$. The kernel r is defined as:

$$r(s) = \begin{cases} a_{70}|s|^7 + \ldots + a_{10}|s| + a_{00}, & |s| \le 1 \\ a_{71}|s|^7 + \ldots + a_{11}|s| + a_{01}, & 1 < |s| \le 2 \\ a_{72}|s|^7 + \ldots + a_{12}|s| + a_{02}, & 2 < |s| \le 3 \\ a_{73}|s|^7 + \ldots + a_{13}|s| + a_{03}, & 3 < |s| \le 4 \\ a_{74}|s|^7 + \ldots + a_{14}|s| + a_{04}, & 4 < |s| \le 5 \\ 0, & \text{otherwise} \end{cases}, \tag{1}$$

The kernel consists of piecewise seventh-order polynomials defined over the subintervals $(-5, -4)$, ..., $(4, 5)$. These polynomials must satisfy the following constraints [12]: a) $r(0) = 1$, b) $r(s) = 0$ for $|s| = 1, \ldots, 5$, and c) the derivatives $r^{(\ell)}(s)$ must be continuous at $|s| = 1, \ldots, 5$, where $\ell = 1, \ldots, 5$. Based on these constraints, a system of 38 equations with 40 unknowns was formulated. To obtain an unambiguous solution to the system, two variables were selected as independent parameters. These variables were defined as $\alpha = a_{73}$ and $\beta = a_{74}$. The solutions of the system, i.e., the coefficients of the 2P kernel defined by Eq. (1), are given in Table I.

Table I. The 40 coefficients of the polynomial seventh-order 2P kernel as functions of α and β

i	a_{7i}	a_{6i}	a_{5i}	a_{4i}
0	$245\alpha - 13909\beta + 821/1734$	$-621\alpha + 35289\beta - 1148/867$	0	$760\alpha - 43280\beta + 1960/867$
1	$301\alpha - 16855\beta + 1687/6936$	$-3309\alpha + 185593\beta - 2492/867$	$14952\alpha - 839958\beta + 32683/2312$	$-35640\alpha + 2005060\beta - 128695/3468$
2	$57\alpha - 2947\beta + 35/6936$	$-1083\alpha + 56295\beta - 175/1734$	$8736\alpha - 456654\beta + 1995/2312$	$-38720\alpha + 2035660\beta - 4725/1156$
3	α	$-27\alpha + 57\beta$	$312\alpha - 1353\beta$	$-2000\alpha + 13360\beta$
4	β	-34β	495β	-4000β
	a_{3i}	a_{2i}	a_{1i}	a_{0i}
0	0	$-384\alpha + 21900\beta - 1393/578$	0	1
1	$47880\alpha - 2696750\beta + 127575/2312$	$-36000\alpha + 2028996\beta - 13006/289$	$14168\alpha - 798714\beta + 120407/6936$	$-2352\alpha + 132628\beta - 2233/1156$
2	$101640\alpha - 5374510\beta + 1575/136$	$-157632\alpha + 8382180\beta - 5670/289$	$133336\alpha - 7127418\beta + 42525/2312$	$-47280\alpha + 2538900\beta - 8505/1156$
3	$7680\alpha - 70225\beta$	$-17664\alpha + 207174\beta$	$22528\alpha - 325119\beta$	$-12288\alpha + 211932\beta$
4	19375β	-56250β	90625β	-62500β

III. OPTIMIZATION OF THE KERNEL PARAMETERS

In [8], the Slope criterion was proposed for the optimization of parameters of polynomial interpolation kernels. The Slope criterion requires the slope of the optimized kernel characteristic at the nodes $s = 1$ and $s = 2$ to be equal to the corresponding slopes of the ideal $sinc$ kernel. Since, by definition, the kernel $r(s)$ in Eq. (1) is a symmetric function, it is sufficient to perform the analysis only at the node $s = 1$. Based on the definition of the 2P kernel given by Eq. (1), the piecewise seventh-order polynomial on the interval $(0, 1)$ is given by:

$$\begin{aligned} r_0(s) = &\left(245\alpha - 13909\beta + \frac{821}{1734}\right)s^7 + \left(35289\beta - 621\alpha - \frac{1148}{867}\right)s^6 \\ &+ \left(760\alpha - 43280\beta + \frac{1960}{867}\right)s^4 + \left(21900\beta - 384\alpha - \frac{1393}{578}\right)s^2 + 1 \end{aligned}. \tag{2}$$

The slope of the kernel time-domain characteristic on the interval $(0, 1)$ is given by:

$$\begin{aligned} \frac{dr_0(s)}{ds} = &7\left(245\alpha - 13909\beta + \frac{821}{1734}\right)s^6 + 6\left(35289\beta - 621\alpha - \frac{1148}{867}\right)s^5 \\ &+ 4\left(760\alpha - 43280\beta + \frac{1960}{867}\right)s^3 + 2\left(21900\beta - 384\alpha - \frac{1393}{578}\right)s \end{aligned}. \tag{3}$$

The slope of the time-domain characteristic at the node $s = 1$ is given by:

$$k_1 = \left.\frac{dr_0(s)}{ds}\right|_{s=1} = 261\alpha - 14949\beta - \frac{707}{1734}, \tag{4}$$

The slope of the ideal $sinc$ kernel is given by:

$$k_{\text{sinc}} = \frac{d}{ds}\text{sinc}(s) = \frac{d}{ds}\left(\frac{\sin(\pi s)}{\pi s}\right) = \frac{\pi s\cos(\pi s) - \sin(\pi s)}{\pi s^2}, \tag{5}$$

The slope of the ideal $sinc$ kernel at the node $s = 1$ is given by:

$$k_{\text{sinc},1} = \left.\frac{d}{ds}\text{sinc}(s)\right|_{s=1} = -1, \tag{6}$$

According to the Slope criterion, the slope of the time-domain characteristic of the 2P kernel at the interpolation node $s = 1$ must be equal to the corresponding slope of the ideal sinc kernel. Therefore, from Eqs. (4) and (6), the following equality is obtained:

$$k_1 = k_{\text{sinc},1} \Rightarrow 261\alpha - 14949\beta - \frac{707}{1734} = -1. \tag{7}$$

Equation (7) contains two unknown parameters, α and β, and therefore cannot be solved uniquely. In other words, infinitely many pairs of values (α, β) can be determined that satisfy Eq. (7):

$$\alpha_1(\beta) = \frac{1661}{29}\beta - \frac{1027}{452574}. \tag{8}$$

To obtain a unique solution, the Slope criterion is extended. According to the Extended slope criterion, in addition to the equality between the slope of the time-domain characteristic of the 2P kernel and that of the ideal $sinc$ kernel at the node $s = 1$, the corresponding slopes at the node $s = 2$ must also be equal. Applying the same procedure to the time-domain characteristic of the 2P kernel on the interval $(1, 2)$, the piecewise seventh-order polynomial $r_1(s)$ and its first derivative $r_1'(s)$ are obtained. Consequently, the slope at the node $s = 2$ is determined as:

$$k_2 = \frac{d}{ds} r_1(s)\bigg|_{s=2} = 4366\beta - 72\alpha + \frac{35}{6936}. \tag{9}$$

The slope of the ideal $sinc$ kernel at the node $s = 2$ is determined from Eq. (5):

$$k_{\text{sinc},2} = \frac{d}{ds}\text{sinc}(s)\bigg|_{s=2} = \frac{1}{2}. \tag{10}$$

According to the Extended slope criterion, the following equality must be satisfied:

$$k_2 = k_{\text{sinc},2} \Rightarrow 4366\beta - 72\alpha + \frac{35}{6936} = \frac{1}{2}. \tag{11}$$

The solutions for α and β satisfying Eq. (11) are:

$$\alpha_2(\beta) = \frac{2183}{36}\beta - \frac{3433}{499392}, \tag{12}$$

To obtain a unique solution for the kernel parameters that satisfies the slope equalities, a system of equations is formed from Eqs. (8) and (12), whose solution gives the optimal values of the kernel parameters α and β:

$$\begin{aligned} \alpha_\zeta &= \frac{33384389}{438341328} \approx 0.0761607151 \approx \frac{146}{1917} \\ \beta_\zeta &= \frac{22231}{16234864} \approx 0.001369337002 \approx \frac{25}{18257} \end{aligned}, \tag{13}$$

Fig. 1.a shows the time-domain characteristic of the $sinc$ kernel, r_{sinc}, windowed using a rectangular (boxcar) window w_{rect} of length $L_w = 40$, i.e., $r_{\text{sincw}} = r_{\text{sincw}} \cdot w_{\text{rect}}$. The amplitude characteristics, calculated using the Fourier transform, ($H_{\text{sincw}} = \mathcal{F}(r_{\text{sincw}})$), are shown in Fig. 1(b) for: a) the ideal $sinc$ kernel ($L_w \to \infty$) and b) windowed $sinc$ kernels with lengths $L_w = 40$, $L_w = 20$, $L_w = 10$, and $L_w = 6$. The logarithmic plots of the amplitude characteristics are shown in Fig. 1.c. Fig. 2.a shows the time-domain characteristics of: a) the windowed $sinc$ kernel, r_{sincw}, with $L_w = 10$; b) the seventh-order 1P kernel, $r_{\zeta,7th,1P}$, with $\alpha_{1P,\zeta} = -1027/452574$ [8]; and c) the seventh-order 2P kernel, $r_{\zeta,7th,2P}$, with $\alpha_\zeta = 146/1917$ and β_ζ=25/18257. Fig. 2.b shows the spectral characteristics of: a) the ideal $sinc$ kernel, H_{sinc}; (b) the windowed $sinc$ kernel, H_{sincw}, with $L_w = 10$; c) the seventh-order 1P kernel, $H_{\zeta,7th,1P}$; and d) the seventh-order 2P kernel, $H_{\zeta,7th,2P}$.

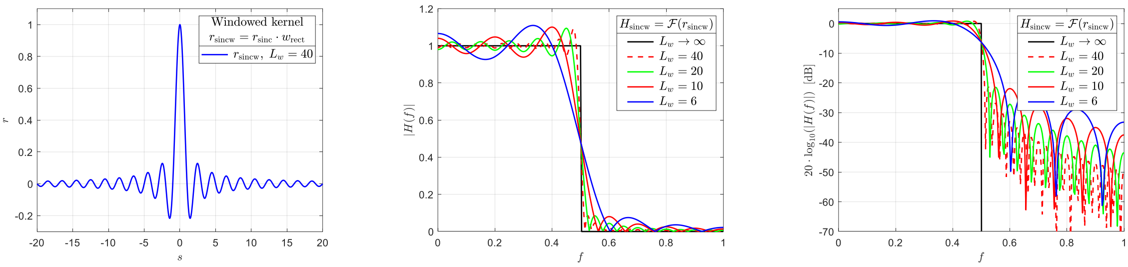

Figure 1. Characteristics of the $sinc$ kernels: a) time-domain characteristic of the windowed $sinc$ kernel r_{sincw}; b) amplitude characteristics of the ideal $sinc$ kernel, H_{sinc}, and the windowed $sinc$ kernels H_{sincw}; and c) logarithmic plots of the amplitude characteristics.

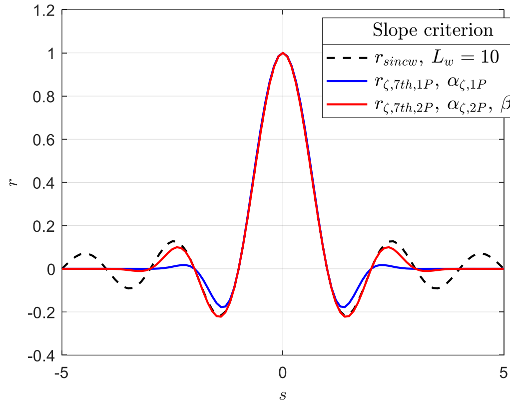

a)

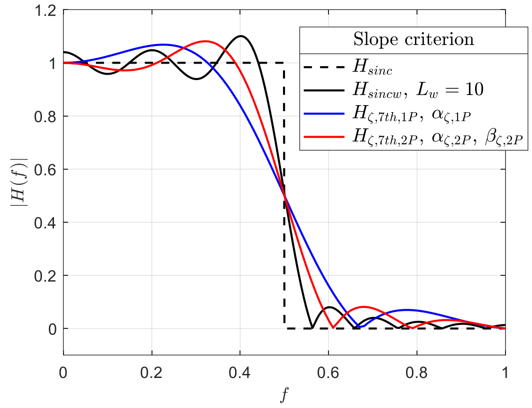

b)

Figure 2. Characteristics of the kernels: a) time-domain characteristics of the windowed $sinc$ kernel, the seventh-order 1P kernel $r_{\zeta 7th,1P}$, with $\alpha_{1P,\zeta} = -1027/452574$, and the seventh-order 2P kernel $r_{7th,2P}$, with $\alpha_\zeta = 146/1917$ and β_ζ=25/18257; and b) spectral characteristics of the ideal $sinc$ kernel H_{sinc}, the windowed $sinc$ kernel H_{sincw}, the seventh-order 1P kernel $H_{\zeta 7th,1P}$, and the seventh-order 2P kernel $H_{\zeta 7th,2P}$.

IV. PERFORMANCE OF THE OPTIMIZED 2P KERNEL

The performance of the seventh-order polynomial 2P interpolation kernel, optimized in the time domain using the Extended slope criterion, is analyzed in the spectral domain. The deviation of the amplitude characteristic of the 2P kernel from the spectral characteristic of the ideal interpolation $sinc$ kernel, H_{sinc}, which is a box function, is analyzed using similarity measures.

Similarity measures

As measures of the deviation of the spectral characteristic of the 2P kernel, $H(f)$, from the box characteristic, H_{sinc}, the following were used: a) the error function $E(f)$; b) the total squared error E_T; c) the slope of the amplitude characteristic $k_H(1/2)$; and d) the ripple of the amplitude characteristic $H_{\text{r}}(f)$.

a) The error function, $E(f)$, represents the squared difference between the amplitude characteristics and is defined as:

$$E(f) = \left|H_{\text{sinc}}(f) - H(f)\right|^2 = \left|1 - H(f)\right|^2 , \tag{14}$$

b) The total squared error, E_T, is defined as the integral of the squared difference between the amplitude characteristics over the passband frequency range:

$$E_T = \int_{-1/2}^{1/2} |1 - H(f)|^2 \,\mathrm{d}f = \int_{-1/2}^{1/2} E(f)\,\mathrm{d}f , \tag{15}$$

c) The slope of the amplitude characteristic, k_H, is defined as the derivative of the amplitude characteristic in the transition band, evaluated at $f = 1/2$:

$$k_H = \left.\frac{\mathrm{d}H(f)}{\mathrm{d}f}\right|_{f=1/2} , \tag{16}$$

d) Ripple characteristic $H_{\text{r}}(f)$. The amplitude characteristic of the kernel, $H(f)$, can be represented as the sum of two components: a smooth (ripple-free) component, $H_{\text{s}}(f)$, and a ripple component, $H_{\text{r}}(f)$:

$$H(f) = H_{\text{s}}(f) + H_{\text{r}}(f) . \tag{17}$$

The smooth component $H_{\text{s}}(f)$ models the underlying monotonically decreasing amplitude characteristic of the kernel. It is obtained by zero-phase FIR filtering, $H_{\text{s}}(f) = LPF\{H(f)\}$. The ripple component $H_{\text{r}}(f)$ exhibits oscillations, or ripples, along the frequency axis f. It is defined as the difference between the amplitude characteristic $H(f)$ and the smooth component $H_{\text{s}}(f)$, i.e., $H_{\text{r}}(f) = H(f) - H_{\text{s}}(f)$. As a measure of the ripple of the amplitude characteristic $H(f)$, several parameters of the ripple component $H_{\text{r}}(f)$ are analyzed, primarily over the passband frequency range $(0, f_c)$:

i) Peak-to-peak ripple:

$$H_{\text{r,pp}} = \max_f H_{\text{r}}(f) - \min_f H_{\text{r}}(f) , \tag{18}$$

ii) Root-mean-square (RMS) ripple:

$$R_{\mathrm{r,rms}} = \mathrm{RMS}\{H_{\mathrm{r}}(f)\} = \sqrt{\frac{1}{2}\int_0^{1/2} H_{\mathrm{r}}^2(f)\,\mathrm{d}f}\,, \tag{19}$$

iii) Ripple energy:

$$E_{\mathrm{r}} = \int_0^{1/2} H_{\mathrm{r}}^2(f)\,\mathrm{d}f\,. \tag{20}$$

Results

Figure 3.a shows the amplitude characteristic of the ideal *sinc* kernel, H_{sinc}, and the error functions, $E(f)$, for the seventh-order polynomial 1P ($E_{\zeta 7th,1P}$, $r_{\zeta 7th,1P}$, $H_{\zeta 7th,1P}$) and 2P ($E_{\zeta 7th,2P}$,$r_{\zeta 7th,2P}$, $H_{\zeta 7th,2P}$) kernels. The 1P kernel was optimized using the Slope criterion, whereas the 2P kernel was optimized using the Extended slope criterion. The corresponding error functions are shown as log-plots in Fig. 3.b. Figure 4.a shows the amplitude characteristic of the ideal *sinc* kernel, H_{sinc}, and the smooth components, H_{s}, of: a) the windowed *sinc* kernel, $H_{\mathrm{s,sincw}}$, $L_w = 10$; b) the seventh-order polynomial 1P kernel, $H_{s,\zeta 7th,1P}$; and c) the seventh-order polynomial 2P kernel, $H_{s,\zeta 7th,2P}$. The corresponding ripple components, $H_{\mathrm{r,sincw}}$, $H_{r,\zeta 7th,1P}$, and $H_{r,\zeta 7th,2P}$, are shown in Fig. 4.b. Table I presents the numerical values of the similarity measures for the optimized seventh-order polynomial 1P and 2P kernels: a) the total squared error, E_T (Eq. (15)); b) the slope of the amplitude characteristic, k_H (Eq. (16)); and the ripple measures: c) peak-to-peak ripple, $H_{\mathrm{r,pp}}$ (Eq. (18)); d) root-mean-square (RMS) ripple, $H_{\mathrm{r,rms}}$ (Eq. (19)); and e) ripple energy, E_r (Eq. (20)). In addition, Table I presents the corresponding similarity measures for the non-parametric kernels: (a) the ideal sinc kernel, r_{sinc}, and (b) the windowed *sinc* kernel, r_{sincw}.

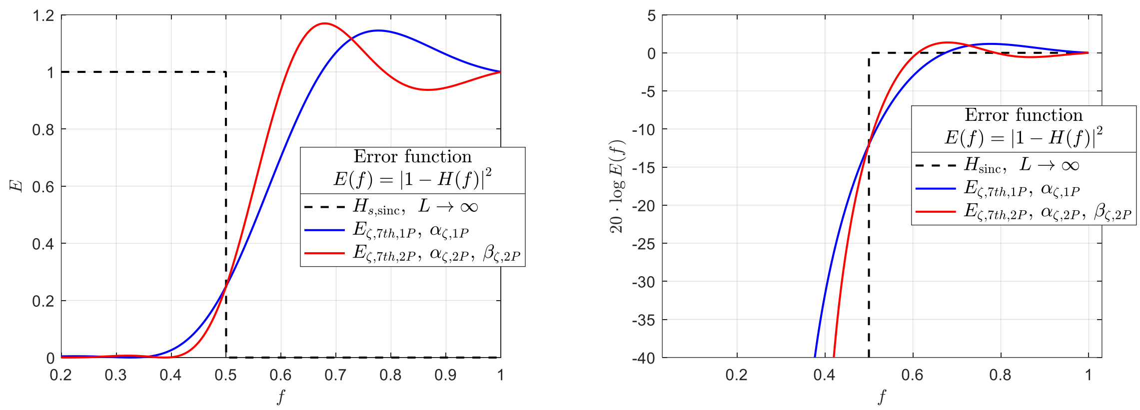

a) b)

Figure 3. a) Amplitude characteristic of the ideal *sinc* kernel, H_{sinc}, and the error functions $E(f)$ of the seventh-order 1P kernel ($E_{\zeta 7th,1P}$,$r_{\zeta 7th,1P}$, $H_{\zeta 7th,1P}$) and the seventh-order 2P kernel ($E_{\zeta 7th,2P}$,$r_{\zeta 7th,2P}$, $H_{\zeta 7th,2P}$);(b) log-plots of the corresponding error functions.

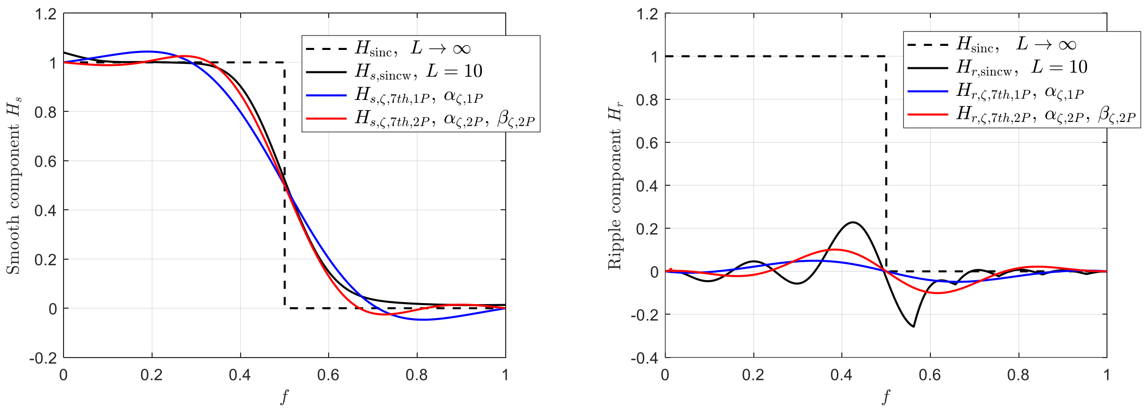

a) b)

Figure 4. a) Amplitude characteristic of the ideal *sinc* kernel, H_{sinc}, and the smooth components, H_{s}, of the windowed *sinc* kernel, $H_{\mathrm{s,sincw}}$, $L_w = 10$, the seventh-order polynomial 1P kernel, $H_{s,\zeta 7th,1P}$, and the seventh-order polynomial 2P kernel, $H_{s,\zeta 7th,2P}$; b) corresponding ripple components, $H_{r,sincw}$, $H_{r,\zeta 7th,1P}$, and $H_{r,\zeta 7th,2P}$.

Table II. Numerical values of the similarity measures.

Kernel	α	β	E_T	$k_H(1/2)$	$H_{r,pp}$	$H_{r,rms}$	E_r
r_{sinc}	-	-	0	∞	0	0	0
r_{sincw}	-	-	0.0201	-9.9916	0.4851	0.0857	0.0074
Extended slope criterion							
	α_ζ	β_ζ	$E_{T,\zeta}$	$k_\zeta(1/2)$	$H_{r,pp,\zeta}$	$H_{r,rms,\zeta}$	$E_{r\zeta}$
$r_{7th,1P}$	-1027/452574	-	0.0501	-3.6923	0.0980	0.0293	8.5589e-04
$r_{7th,2P}$	146/1917	25/18257	0.0337	-5.6156	0.2022	0.0515	0.0026

Analysis of the Results

Based on the results shown in Table II, it can be concluded that, with the applied Extended slope criterion for optimizing the parameters of the seventh-order polynomial 2P kernel, the total squared error E_T is: a) higher than that of the windowed sinc kernel ⇒ $E_{T,\text{sincw}}/E_{T,\zeta 7rd,2P} = 0.0201/0.0337 = 0.5964$, i.e., $E_{T,\zeta 7rd,2P}$ is approximately 1.68 times higher than $E_{T,\text{sincw}}$; b) lower than that of the seventh-order 1P kernel ⇒ $E_{T,\zeta 7rd,1P}/E_{T,\zeta 7rd,2P} = 0.0501/0.0337 = 1.4866$, i.e., $E_{T,\zeta 7rd,1P}$ is 1.4866 times higher than $E_{T,\zeta 7rd,2P}$.

The slope k_H of the spectral characteristic of the seventh-order polynomial 2P kernel in the transition band, when the optimization is performed in accordance with the Extended slope criterion, is: a) lower than that of the windowed sinc kernel ⇒ $k_{H,\zeta 7rd,2P}/k_{H,\text{sincw}} = 5.6156/9.9916 = 0.5620$, i.e., the slope of the seventh-order 2P kernel is approximately 1.78 times lower than that of the windowed sinc kernel; b) higher than that of the seventh-order 1P kernel ⇒ $k_{H,\zeta 7rd,2P}/k_{H,\zeta 7rd,1P} = 5.6156/3.6923 = 1.5209$, i.e., the slope of the seventh-order 2P kernel is 1.5209 times higher than that of the seventh-order 1P kernel.

The analysis of the ripple of the spectral amplitude characteristic H leads to the following conclusions.

i) The peak-to-peak ripple $H_{\text{r,pp}}$ of the seventh-order 2P kernel is: a) lower than that of the windowed sinc kernel ⇒ $H_{r,pp,\text{sincw}}/H_{r,pp,\zeta 7rd,2P} = 0.4851/0.2022 = 2.3991$, i.e., the peak-to-peak ripple of the windowed sinc kernel is 2.3991 times higher than that of the seventh-order 2P kernel; b) higher than that of the seventh-order 1P kernel ⇒ $H_{r,pp,\zeta 7rd,1P}$ / $H_{r,pp,\zeta 7rd,2P} = 0.0980/0.2022 = 0.4847$, i.e., the peak-to-peak ripple of the seventh-order 2P kernel is approximately 2.06 times higher than that of the seventh-order 1P kernel.

ii) The root-mean-square (RMS) ripple $H_{\text{r,rms}}$ of the seventh-order 2P kernel is: a) lower than that of the windowed sinc kernel ⇒ $H_{r,rms,\text{sincw}}/H_{r,rms,\zeta 7rd,2P} = 0.0857/0.0515 = 1.6641$, i.e., the RMS ripple of the windowed sinc kernel is 1.6641 times higher than that of the seventh-order 2P kernel; b) higher than that of the seventh-order 1P kernel ⇒ $H_{r,rms,\zeta 7rd,1P}$ / $H_{r,rms,\zeta 7rd,2P} = 0.0293/0.0515 = 0.5689$, i.e., the RMS ripple of the seventh-order 2P kernel is approximately 1.76 times higher than that of the seventh-order 1P kernel.

iii) The ripple energy E_r of the seventh-order 2P kernel is: a) lower than that of the windowed sinc kernel ⇒ $E_{r,\text{sincw}}/E_{r,\zeta 7rd,2P} = 0.0074/0.0026 = 2.8462$, i.e., the ripple energy of the windowed sinc kernel is 2.8462 times higher than that of the seventh-order 2P kernel; b) higher than that of the seventh-order 1P kernel ⇒ $E_{r,\zeta 7rd,1P}$ / $E_{r,\zeta 7rd,2P} = 8.5589e-04/0.0026 = 0.3292$, i.e., the ripple energy of the seventh-order 2P kernel is approximately 3.04 times higher than that of the seventh-order 1P kernel.

The comparative analysis demonstrates that the seventh-order polynomial 2P interpolation kernel optimized using the Extended slope criterion has a lower total squared error and lower ripple measures than the windowed sinc kernel, indicating a closer approximation to the ideal box characteristic in these respects. However, the slope of the amplitude characteristic of the optimized 2P kernel in the transition band is lower than that of the windowed sinc kernel. Compared with the seventh-order polynomial 1P kernel, the optimized 2P kernel exhibits a lower total squared error and a higher transition-band slope, indicating improved spectral similarity in these respects. However, all considered ripple measures of the 2P kernel are higher than those of the 1P kernel.

These results demonstrate that the introduction of an additional parameter and its optimization using the Extended slope criterion improves selected spectral characteristics of the polynomial interpolation kernel, although a trade-off remains between the transition-band slope, total squared error, and ripple behavior.

Further optimization of the seventh-order polynomial 2P kernel will be considered using the Continuity criterion. This criterion will impose an additional condition requiring the $(n-1)$th derivative of the kernel at the corresponding interpolation nodes to match the corresponding derivative of the ideal sinc kernel, with the aim of further improving the spectral characteristics of the optimized interpolation kernel.

V. CONCLUSION

The polynomial seventh-order two-parameter 2P interpolation kernel was optimized using the Extended slope criterion. The Extended slope criterion extends the conventional Slope criterion by imposing slope-matching conditions at the interpolation nodes $s = 1$ and $s = 2$, resulting in a unique pair of optimal kernel parameters α and β. The spectral analysis shows that the optimized 2P kernel has a lower total squared error and lower ripple measures than the windowed sinc kernel, but a lower transition-band slope. Compared with the seventh-order polynomial 1P kernel, the optimized 2P kernel exhibits a lower total squared error and a higher transition-band slope, but higher ripple measures. These results demonstrate that the additional kernel parameter provides greater flexibility in balancing spectral approximation error, transition-band slope, and ripple behavior. Further optimization of the seventh-order 2P kernel will focus on the Continuity Criterion, based on matching the $(n-1)$th derivative of the polynomial kernel at the corresponding interpolation nodes to the derivative of the ideal sinc kernel.

REFERENCES

[1]. A. Kazuyuki, K. Shoichi and S. Hiroshi. Spatial active noise control based on individual kernel interpolation of primary and secondary sound fields. IEEE International Conference on Acoustics, Speech, and Signal Processing (ICASSP), 2022, 1056–1060.

[2]. R. Keys. Cubic convolution interpolation for digital image processing. IEEE Transactions on Acoustics, Speech, and Signal Processing, 29(1), 1981, 1153–1160.

[3]. B. Sun and S. Xin. An edge-guided weighted image interpolation algorithm. 2023 IEEE 13th International Conference on Electronics Information and Emergency Communication (ICEIEC), Beijing, China, 2023, 139–143.

[4]. O. Rukundo and B. Maharaj. Optimization of image interpolation based on nearest neighbor algorithm. International Conference on Computer Vision Theory and Applications (VISAPP), Lisbon, Portugal, 2014, 641–647.

[5]. Z. Guo, Q. Wang, J. Du, J. Pan, Q.-F. Liu and C.-H. Lee. A variance-preserving interpolation approach for diffusion models with applications to single-channel speech enhancement and recognition. IEEE/ACM Transactions on Audio, Speech, and Language Processing, 32, 2024, 3025–3038.

[6]. M. Maczka, S. Pawłowski and G. Hałdaś. Application of polynomial approximation in simulations of quantum cascade lasers. Przegląd Elektrotechniczny, 98(12), 2022, 321–324.

[7]. E. Meijering. A chronology of interpolation: From ancient astronomy to modern signal and image processing. Proceedings of the IEEE, 90(3), 2002, 319–342.

[8]. J. Niessen, E. Meijering, J. Pluim and A. Viergever. Quantitative comparison of sinc-approximating kernels for medical image interpolation. Lecture Notes in Computer Science, 1679, 1999, 210–217.

[9]. J. Shangguan, L. Yan and W. Yong. Fast algorithm of modified cubic convolution interpolation. 4th IEEE International Congress on Image and Signal Processing, 2011, 1072–1075.

[10]. E. Meijering and M. Unser. A note on cubic convolution interpolation. IEEE Transactions on Image Processing, 12(4), 2003, 477–479.

[11]. N. Savić, Z. Milivojević and B. Prlinčević. Development of the 2P fifth-degree interpolation convolutional kernel. International Journal of Innovative Research in Advanced Engineering (IJIRAE), 11(8), 2021, 306–311.

[12]. Z. Milivojević, N. Savić, B. Prlinčević, V. Stojanović and D. Kostić. Construction and Parameterization of a Polynomial Seventh-Order Two-Parameter Interpolation Kernel. International Refereed Journal of Engineering and Science (IRJES), 15(4), 2026, 86–92.

[13]. K. Meijering, M. Zuiderveld and A. Viergever. Image reconstruction by convolution with symmetrical piecewise n-th-order polynomial kernels. IEEE Transactions on Image Processing, 8(2), 1999, 192–201.